Two-dimensional Monte Carlo simulations of ionic and nonionic silane self-assembly on hydrophilic surfaces

Vivek Kapila,[a] A. Marcia Almanza-Workman, Pierre A. Deymier, and Srini Raghavan
Department of Materials Science and Engineering, University of Arizona, Tucson, Arizona 85721

(Received 17 November 2003; accepted 25 February 2004)

Aqueous chemistries have recently been shown to be useful for the deposition of hydrophobic films of nonionic and cationic silanes on hydrophilic substrates for the prevention of *stiction* in MEMS. The Monte Carlo method is used to simulate in two dimensions the self-assembly of silane films on a hydrophilic surface. We investigate the impact of charged group in cationic silane on the overall structure of the films. We characterize the film structure with spatial pair correlations at each molecular layer of the deposited films. The simulations reveal long-range correlations for the film of cationic silanes. Based on our two-dimensional simulations, we report an average ''most probable'' structure for the films of nonionic and cationic silanes. © *2004 American Institute of Physics.* [DOI: 10.1063/1.1710859]

INTRODUCTION

Surface micromachining is a widely used technique for fabricating microelectromechanical devices used in various applications. During wet etch processing, the microstructures may collapse due to very strong capillary forces between the wet, hydrophilic polysilicon surfaces. This is often termed as ''stiction.''[1–3] Among the most successful approaches to prevent the stiction problem is one involving chemical modification of the surfaces to render them hydrophobic. This is usually achieved by deposition of organic silanes on oxidized polysilicon surfaces. Traditionally, a long-chain silane is deposited from an organic solution.[1,4,5] To address the rising concerns about organic wastes in the work place, research efforts have also been directed towards the development of efficient coating methods utilizing aqueous chemistries.[6–9]

Recently, commercially available water dispersible nonionic and cationic silanes have been shown to result in highly hydrophobic films on a hydrophilic substrate.[8,9] However, the deposited films, characterized by the electrochemical impedance spectroscopy (EIS), were found to be more porous in the case of cationic silane than in the case of the nonionic silane.[9] A higher porosity in the cationic silane films is hypothesized to be caused by the presence of a cationic group in the silane chain. However, a molecular level study of these films is not available. Atomistic simulation techniques, such as Monte Carlo (MC) and molecular dynamics (MD) can provide a window at the molecular level for investigating the bulk silane solutions and silane films.

Monte Carlo (MC) and molecular dynamics (MD) methods have been used successfully in the past to study the chemical systems and the self-assembled monolayers comprising surfactant molecules. Surfactants are organic molecules similar to alkyl silane except that the head group in the surfactant is not reactive unlike the head group in a silane.

Molecular dynamics (MD) simulations have successfully been used to study the morphology of monolayers of the cationic surfactant cetyltrimethylammonium bromide (C_{16}TAB) at the interface between a hydrophobic substrate and an aqueous solution.[10] Also, dynamic properties, such as, the average orientation angle of the hydrophobic chains of monododecyl pentaethylene glycol ($C_{12}E_5$) monolayers have been investigated at the water surface[11] using MD technique.

Simulations have also been used as means for proposing the mechanisms of the surfactant adsorption and aggregation using simple description of molecules and interfaces.[12] The models based on harmonic potentials and the Lennard-Jones (LJ) potentials have been shown to capture, at least qualitatively, the basic characteristics of water/solid interfaces and micellar solutions, and how they are influenced by the concentration and structure of surfactant molecules.[12]

Zhang *et al.*[13] used molecular mechanics and molecular dynamics simulations to find the optimal packing structure of C_{18} alkyl monolayers on a Si(111) surface. The force fields used for the alkyl/Si(111) system were verified by *ab initio* quantum chemical calculations. It was shown that the optimal packing structure was size independent when it was extended to large systems. Also, an investigation of alkylsilane monolayers on silica surface has been reported, recently.[14]

Monte Carlo simulations have been used to study the self-assembly of model surfactants on hydrophilic[15] and hydrophobic surfaces,[16] and also self-assembly of alkanethiol on Au(111).[17] These simulations have provided the phase and structural behavior of the model system as a function of temperature, coverage, and the magnitude of surface corrugation.

In this paper, we have developed coarse-grained models in two dimensions for the aqueous solutions of cationic and nonionic silanes. The choice of two-dimensional (2D) models was based on the ease in modeling and ease in computations. These models are used for studying the structure of self-assembled monolayers of silanes on polysilicon surfaces using Monte Carlo simulations. Coarse-grained models greatly simplify the physical description of the system and

[a]Author to whom correspondence should be addressed. Electronic mail: vkapila@email.arizona.edu

prove very useful for rapid sampling of phase space. Such coarse-grained models have been used successfully in the pioneering MC simulations of Larson,[18–22] and MD simulations of Smit.[23–25] Recently, coarse-grained methods have also been used for membrane studies by Klein and co-workers[26] and Marrink and co-workers.[27]

Although the lattice models are highly simplified, they still capture in many cases the essential physics of the processes occurring at the molecular level. Lattice models are particularly useful in the examination of systems consisting of long-chain molecules such as ours. Wide ranges of time and length scales are required to adequately describe the behavior of long-chain molecules. The time scales range from approximately 10^{-14} s (i.e., the period of a bond vibration) through seconds, hours, or even longer, e.g., time for molecular diffusion and self-assembly. The size scales range from angstroms to nanometers to micrometers (e.g., length of the polymer to spatial extent of aggregates of molecules). The lattice models allow spatial coarse graining of these features. The MC methods enable various moves without reference to their hierarchy of relaxation time. In coarse-grained MC, therefore, many states can be generated rapidly and analyzed.

The paper is organized as follows. In Sec. II, we describe the cationic and nonionic silane models used in the present study. The results obtained from the simulations are described in Sec. III using head and tail group distribution profiles as a function of distance from the surface and spatial pair correlations at each layer of the film. Finally, we conclude the paper with a brief summary of the findings of the work in Sec. IV.

SIMULATION MODEL AND PROCEDURE

In a previous work,[28] we modeled and simulated the aggregation behavior of coarse-grained models of surfactant molecules in aqueous solutions. The silane molecules have a chainlike structure similar to the surfactant molecules, and both have a hydrocarbon backbone. Because of this structural similarity in silane and surfactant molecules we model the silane molecules based on our previous surfactant model. However, some modifications to the previous model are necessitated because of the inherent differences in the nature of the head groups in silanes and surfactants. In contrast to surfactant molecules, silanes consist of a reactive head group that can lead to polymerization reactions. Also, interactions are included between the surface sites and the chemical groups in the silane for simulating the deposition of silane films on solid substrate.

The cationic and nonionic silane molecules are modeled as chains of connected grid sites on a 2D square lattice. Each nonionic silane chain consists of one hydrophilic head group and 12 hydrophobic tail groups. The cationic silanes consist of a hydrophilic head group (nonionic), 11 hydrophobic tail groups and a cationic group. It must be noted here that the cationic silane used in the experiments[9] contains a $(-CH_2)_n$ segment, known as spacer, between the hydrophilic head group and the cationic group. Given that the chemical groups in the spacer and the hydrophobic tail are the same $(-CH_2)$, no distinction has been made between them and both are referred to as the tail groups. Figures 1(a) and 1(b) show the representation of nonionic and cationic silane chains on a 2D square grid lattice, respectively.

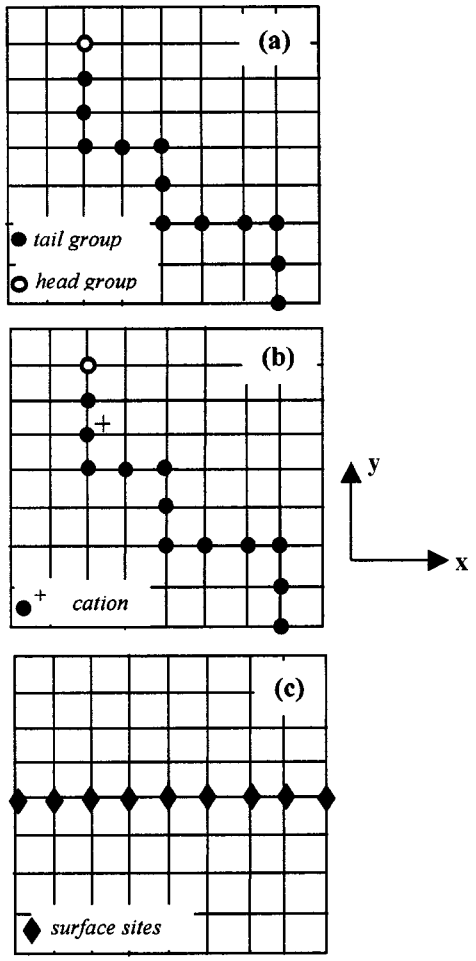

FIG. 1. Representation of (a) nonionic silane, (b) cationic silane, (c) surface sites on the 2D square grid lattice.

A one-dimensional model has been used for the hydrophilic surface. The grid sites $(x \in [1,L], y = L/2)$ represent the surface sites on the hydrophilic substrate in a simulation cell of size $(L \times L)$. Under the conditions of experiments,[8,9] the pH of the silane solution is maintained at ~ 4. This results in a distribution of –OH and negatively charged O^- terminated sites on the hydrophilic surface. The hydrophilic head groups of silane chemisorb at the –OH terminated surface sites whereas cationic groups electrostatically physisorb to the O^- terminated sites. Generation of a realistic distribution of –OH, and O^- terminated sites in the surface model would necessitate simulation of large system sizes imposing a computational load difficult to attain on our available computer platforms.

Therefore, in our model we assume all the surface sites to be –OH terminated and we make a mean field approximation for the surface charges by distributing them uniformly across the entire surface. The choice of mean field approximation for surface charges is similar to the Gouy–Chapman treatment of surface charges frequently employed in the studies of surfaces.[29,30] All the surface sites are, therefore, capable of both chemisorbing the hydrophilic head groups and

TABLE I. Summary of chain structure and interaction energies used in nonionic and cationic silane models.

Model	H[a]	T[b]	Pos.[c]	ϵ_{ww}[d]	ϵ_{WH}[d]	ϵ_{WT}[d]	ϵ_{HH}[d]	ϵ_{HT}[d]	ϵ_{TT}[d]	ϵ_{II}[d]	ϵ_{SH}[d]	ϵ_{ST}[d]	ϵ_{SI}[d]
Nonionic silane	1	12	×	0	−4.44	0.77	−15.0	0.77	0	0	−15.0	1.55	0
Cationic silane	1	12	3	0	−4.44	0.77	−15.0	0.77	0	5.33	−15.0	1.55	−5.33

[a]H, number of head groups.
[b]T, number of tail groups.
[c]Pos., position of ionic group in the chain counting from the head group to the terminal tail group, × indicates no ionic groups in the chain.
[d]ϵ_{ij}'s, the interaction energy values (as multiples of k_BT units) between different pairs of groups.

interacting electrostatically with the cationic groups. In a simulation box of size $(L\times L)$ containing N chains of silane, $13\times N$ sites are occupied by the silane molecules, and L sites are occupied by the surface. The remaining $\{(L\times L)$-$(13\times N)$-$L\}$ empty grid sites are considered to be water sites.

The energy model consists of nearest neighbor short-range interactions between pairs of nonionic groups and long-range Coulomb interactions between the pairs of charged groups. Representing water by W, head group by H, tail group by T, and surface sites by S, the following pair interactions are included, ϵ_{WT}, ϵ_{WH}, ϵ_{HT}, ϵ_{HH}, ϵ_{SH}, ϵ_{ST}. The interactions between a pair of cationic groups of two different chains, and between a cationic group in silane and charged surface sites are described by following Coulomb type interaction,

$$U_{\text{long-range}}=\Sigma_{pairs}\phi/d, \tag{1}$$

where ϕ is the Coulombic interaction between two charged groups separated by a unit grid distance and d is the distance between the charged groups. As charged groups do not see others across the surface, no long-range interaction is calculated between the charged groups across the surface.

Usually, the long-range Coulomb potentials are calculated using Ewald sums method. However, Ewald sums are also known to be computationally very expensive for systems with two-dimensional periodicity. It has been shown that accuracy in the calculation of Coulomb potentials is not significantly sacrificed by employing a truncation at reasonably large distances.[31–33] Also, a truncated Coulomb potential provides at least a twofold enhancement in computational speed compared to the Ewald sums method.[32,33] Based on this we elect to use the truncation method with a cutoff distance of 30 grid units, which was used with success in our previous work on surfactants.[28]

The total energy of the system is, therefore, given by the following expression:

$$U=(\epsilon_{WT}\cdot n_{WT}+\epsilon_{WH}\cdot n_{WH}+\epsilon_{TH}\cdot n_{TH}+\epsilon_{HH}\cdot n_{HH}+\epsilon_{SH}\cdot n_{SH}+\epsilon_{ST}\cdot n_{ST})+U_{\text{long-range}}, \tag{2}$$

where ϵ_{WT}, ϵ_{WH}, ϵ_{TH}, ϵ_{HH}, ϵ_{SH}, and ϵ_{ST} are the interaction energy values between different pairs of chemical groups, and n_{WT}, n_{WH}, etc., are the number of pairs of water-tail, water-head group, and so on. The values of interaction energies used in the simulations are given in Table I.

Owing to the similarity between surfactant and silane structures the interaction energies ϵ_{WT}, ϵ_{TH}, and ϵ_{WH} have been taken from our previous work on surfactants.[28] The reactive head groups in silanes are believed to cause polymerization in the aqueous environment. Therefore, a very strong short-range nearest neighbor attractive interaction, ϵ_{HH}, is assumed between the head groups. To mimic chemical bonding, a value for ϵ_{HH} was chosen empirically as the smallest energy that leads to polymerization of nonionic silane in the bulk solutions in the long time limit. In our simulations, polymerization is said to occur when the head groups of two silane chains are nearest neighbors. Commercial cationic silane solutions used for coating applications consist of silane chains with a cationic group along the silane backbone and mobile counter ions. To enable simulations of the system without explicitly including the counter ions in the solution, we lump the negative charge of the counter ions and the positive charge on the cationic group in silane chains in a single effective interaction energy term ϵ_{II} representing a screened interaction.

To reproduce the dispersed ionic silane solutions, as seen in experiments,[8,9] interaction energy ($\epsilon_{II}=5.3k_BT$) is chosen such that it produces a dispersed bulk solution. To simulate the chemisorption of silane on the (–OH) terminated hydrophilic surface sites, the model employs the same strong nearest neighbor attractive interaction (ϵ_{SH}) between the silane head groups and the surface sites as the head–head interaction (ϵ_{HH}). The hydrophobic tail groups have a short range nearest neighbor repulsive interaction (ϵ_{ST}) with the surface sites. Finally, the interactions (ϵ_{II}) between the cationic groups of different chains are long-range repulsive and the interactions (ϵ_{SI}) between the cationic groups and the charges on the surface sites are long-range attractive. Interaction energy between the water molecules is considered to be zero. All the interactions are relative to water–water interaction. Therefore, the repulsive interactions, ϵ_{WT}, ϵ_{HT}, ϵ_{ST}, ϵ_{II} are positive and attractive interactions ϵ_{WH}, ϵ_{HH}, ϵ_{SH}, ϵ_{SI} are negative.

All the simulations have been run in a constant (N,V,T) ensemble with periodic boundary conditions. First, N_{ch} number of chains is introduced in the simulation cell. The energy of the random configuration is calculated from Eq. (2). The silane chains are then allowed to make Monte Carlo moves on the grid. Four types of MC moves have been used in the simulations; forward reptation, backward reptation, global chain translation, global cluster translation. A cluster is defined as a group of chain molecules sharing nearest neighbor sites. The move is always accepted if it results in a decrease in the overall energy of the system. If the move results in an

increase in the energy then the new configuration is either accepted or rejected on the basis of a transition probability, given by $\exp(-\Delta U/k_BT)$. Here, $\Delta U(=U_{\text{new}}-U_{\text{old}})$ is the difference between the overall energies of new and old configurations. Additionally, a configurational-bias regrowth scheme[34] has been used in which a randomly selected chain molecule is completely regrown from a randomly selected position along the chain. The configurational bias move is particularly important after the adsorption of the chain molecules on the surface when it is not possible to explore the phase space any further with the other conventional MC moves. The simulations are run for 50–100 millions of MC steps following the thermal equilibration.

RESULTS AND DISCUSSIONS

MC simulations have been used to study the self-assembly of ionic and nonionic silane chains on the hydrophilic surface and to examine the structure of the deposited films. Simulations have been run for three different starting concentrations, specifically, $N_{\text{ch}}=120$, 220, and 300. The MC simulations have been run in simulation cell of size 128×128. Because of the periodic boundary conditions, for the hydrophilic surface located at $(x\in[1,128],y=64)$, a maximum of 256 silane chains can attach to the surface sites with their head groups located at $(x\in[1,128],y=63)$ and at $(x\in[1,128],y=65)$. Therefore, the chosen concentration range allows us to explore the self-assembly of silane both below and above the concentration needed for the complete surface coverage.

Two separate procedures are used for film formation depending on the ionicity of the silanes. Cationic silanes are known to remain polydispersed over long periods of time. Owing to the stability of the cationic silane solutions and to simulate the long-time limit solution state, the cationic silane solutions are thermalized for 2–5 million MC steps starting from an initial random configuration. During thermalization, silane chains are inhibited from occupying the surface sites by employing highly repulsive, short-range interaction energies for *HS*, *TS*, and *IS* pairs. Because of the repulsive Coulombic interactions, the cationic silane solution remains polydispersed with the formation of only a few small nonpolymerized aggregates. Since the solution remains essentially polydispersed prior to deposition, the film structure is insensitive to the thermalization. Following this, the interaction energies given in Table I are used for the self-assembly of the silane molecules on the hydrophilic surface. Under experimental conditions, there exist kinetic constraints on the formation of polymerized clusters of nonionic silane. Therefore, nonionic silane solution can remain polydispersed for a small period of time prior to film deposition. Equilibrium MC simulations with multiple time scale moves, such as ours, do not impose any kinetic constraints on the polymerization. Therefore, to avoid the effects of this unrealistic clustering/polymerization on the film structure, the nonionic silanes are allowed to self-assemble on the surface, without prior thermalization, from an initial random, polydispersed configuration employing the interaction energies given in Table I.

Following the self-assembly of ionic/nonionic silane chains on the surface, 50–100 million MC steps are used for the relaxation of the deposited films. After the relaxation of the deposited films, the following structural features are observed (a) silane chains with the head groups attached to the surface sites, (b) polymerized silane chains (i.e., group of silane chains in which head groups of chains share nearest neighbor sites), with the head group of at least one chain in the polymer attached to a surface site, and (c) chains in which head group is neither attached to a surface site nor polymerized with a chain that has its head groups attached to a surface site. The first two types of silane are referred to as the chemisorbed and the last type is referred to as the physisorbed. In actual experiments, the physisorbed silane chains are known to be easily removed from the deposited films in the rinsing operations following film deposition. To simulate the rinsing of the deposited films the physisorbed silane chains are identified and removed from the simulation box. The number of chains that remain chemisorbed on the surface (following the removal of physisorbed chains) in systems of different initial concentrations is given in Table II. It can be seen that in rinsed systems the initial concentration has little impact on the concentration of chemisorbed silane. This indicates that even at the lowest concentration used in the simulations, the surface is saturated with the silane molecules. Following rinsing, the films of ionic and nonionic silane are relaxed for 10–50 million MC steps and the structure of the relaxed films is investigated. For illustration, we show in Fig. 2 snapshots of films formed with nonionic and cationic silanes on the hydrophilic surface in our 2D simulations.

TABLE II. Number concentration of silane chains before and after rinsing.

Starting number concentrations of nonionic and ionic silane chains	Number concentrations after rinsing	
	Nonionic silane	Ionic silane
120	119	114
220	130	108
300	122	113

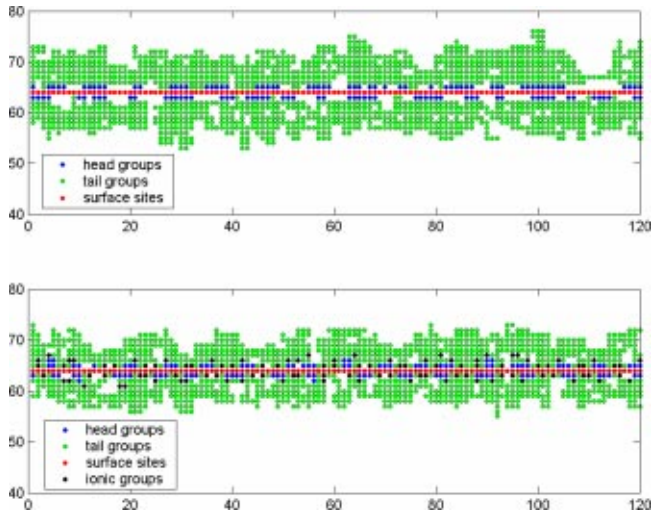

FIG. 2. Snapshots of the (a) nonionic and (b) cationic silane films following rinsing and relaxation.

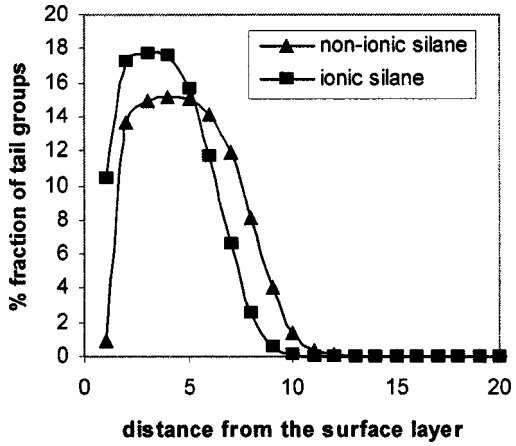

FIG. 3. Distribution profiles of the tail groups (in rinsed and relaxed films) as a function of distance from the hydrophilic surface.

Snapshots are not sufficient to characterize unambiguously the structure of deposited films. Therefore, to gain deeper understanding of the structure of the rinsed and relaxed films, we calculate (a) the head and tail distribution profiles perpendicular to the surface sites as a function of distance from the surface sites, and (b) spatial correlations of different pairs of groups along the surface. Figure 3 shows the tail group profiles as a function of distance from the surface. The tail-group profiles show a larger fraction of tail groups attached to the surface in case of cationic silane than in the case of nonionic silane. These results appear to be the effect of the ionic groups bonding to the surface sites. The hydrophilic head groups of silane attach to the surface because of strong (ϵ_{SH}) interaction, representative of the chemisorption of silane head groups on hydrophilic sites. The ionic groups attach to the surface sites due to the electrostatic interaction. The tail group (or spacer) between the head group and the ionic group, therefore, occupies the surface sites due to the constraints imposed by the square grid lattice. Also, additional hydrophobic groups in the tail attach to the surface sites to screen the electrostatic repulsion between the cationic groups physisorbed on the surface. This leads to a high fraction of tail groups staying in proximity to the surface sites in ionic silane. This also results in fewer water groups attaching to the surface sites in the case of ionic silane.

From Fig. 3, it can also be seen that a higher fraction of tail groups is present in the layers of the ionic–silane films closer to the surface. This indicates that the cationic silane films are more hydrophobic than nonionic films. Experimentally, hydrophobicity is measured in terms of contact angles; higher contact angles representing more hydrophobic surfaces. The structure of our simulated films is therefore consistent with the higher contact angles ($104°\pm2°$ for cationic silane, $87°\pm1°$ for nonionic silane) observed in experiments for the cationic silane films.[35] Also, Fig. 3 shows that the nonionic silane films have a higher thickness than the ionic–silane films which is also consistent with the experimental observations.[35] Since, following rinsing only the chemisorbed silane chains remain in the system (with the head groups of most of these chains attached to the surface sites), distribution profiles for the head groups have not been plotted. However, we must mention here that only ~95% of head groups are attached to the surface sites in the case of ionic silane compared to 100% attachment in the case of nonionic silane. This difference is due to the fact that fewer surface sites are available for head group attachment in case of ionic–silane in which ionic groups and spacer groups also occupy surface sites. The head groups of the remaining 5% chains are bonded to the head groups of the chains chemisorbed on the surface.

To obtain the correlations of different pairs of groups along the surface, we calculate the MC average number of pairs of AB (A, $B=H$, T, and W), as a function of separation distance between A and B, on each layer of the film. The layers are numbered from 0 for the layer occupied by the surface sites. Subsequently, these averages are converted to fractions following Eq. (3):

$$R^i_{AB}(d)=\frac{\langle N^i_{AB}(d)\rangle}{\Sigma_B\langle N^i_{AB}(d)\rangle}. \tag{3}$$

In the above equation, $R^i_{AB}(d)$ represents the fraction of pair AB (e.g., $A=H$, and $B=W$, $AB=HW$) on layer i when the distance between A and B is d grid units. $\langle N^i_{AB}(d)\rangle$ represents the average number of pairs AB on layer i for a separation distance of d, and $\Sigma_B\langle N^i_{AB}(d)\rangle$ is the sum of all the AB pairs, e.g. ($A=H$, $B=H$, T, W, and I), at separation d on layer i.

For the illustration of our method, we first create two model structures: (A) a layer with all the sites occupied by the head groups and (B) a layer with periodically alternating clusters of head and tail groups, $HHHHTTTTHHHHTTTT$, etc., with a period of 8 grid units. In Figs. 4(a) and 4(b), we represent the calculated HH and HT correlations for the model structures (A) and (B), respectively. In Fig. 4(a), as the % fraction of HH pairs at all the distances is 100, therefore, the probability of finding a head group at any distance from any other head group is 1.

In contrast, in Fig. 4(b) we observe that the fractions of both HH and HT correlations at a distance of 1 grid unit are nonzero and fraction of HH correlations is greater than HT correlations. This indicates that there are more HH pairs than the HT pairs. Also, the positions of maxima in the HH correlations indicate that the probability of finding a head group at a distance of 8, 16, 24 grid units from any other head groups is 1. This is consistent with the periodicity of structure used to calculate these correlations.

Arguments similar to those used above in explaining the example structures can be used to understand the more complicated structure of self-assembled films of silane obtained in the MC simulations. As already mentioned, three starting concentrations ($N_{ch}=120$, 220, and 300) were used in these simulations. In this paper, we report only the correlations obtained from systems with starting concentrations of $N_{ch}=220$. Similar correlations have been obtained for other concentrations.

In Figs. 5(a) and 5(b) we show the correlations for HH, HT, HW, and HI on layer 1 for the nonionic and ionic silanes, respectively. The following three observations are

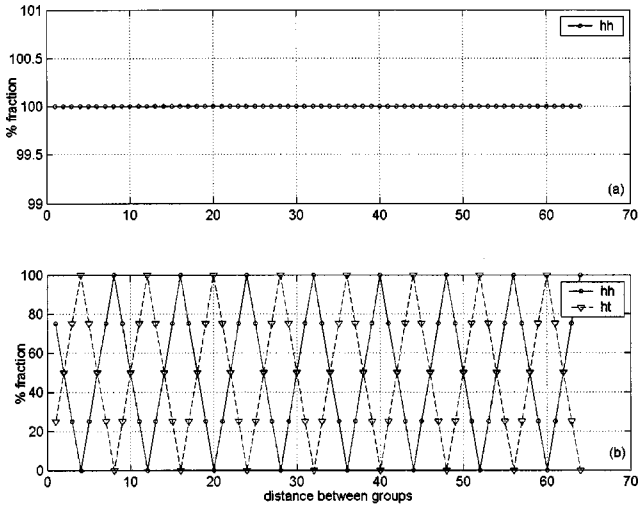

FIG. 4. (a) Sample *HH* correlations for a layer completely occupied by head groups, (b) sample *HH* and *HT* correlations for a layer occupied by head and tail groups in an ordered form.

made from these plots (i) a much higher fraction of *HW* pairs is seen on layer 1 for a nonionic silane compared to the ionic silane, (ii) much higher fractions of tail groups on the layer 1 in ionic silane, and (iii) the pseudoperiodicity of correlations for various paired groups in the ionic and nonionic silane.

The observations (i) and (ii) above are consistent with the observations from the head and tail group profiles obtained perpendicular to the surface layer. The periodicity of correlations between different groups can be used to construct an average picture of the film on the layer 1. Maxima are observed in the *HH* correlations in ionic silane [Fig. 5(b)] at distances of 1, 7, 15, 23 grid units and so on, indicating a high probability of finding a head group at these separation distances from any other head group. Similarly, we also notice maxima in (a) *HI* correlations at distances 3, 10, 18, (b) in *HT* correlations at distances 5, 9, and (c) in *HW* correlations at distances 4, 11, and so on. The positions of the maxima in the plots in Fig. 5(b), therefore, suggest the following average structure of ionic–silane on the layer 1:

$$\underline{HH}TI\underline{WI}T\underline{HHH}TI\underline{WI}T\underline{HH}TI\ldots.$$

The above structure indicates that the head groups are most likely to attach to the surface in pairs of 2–3. The distance between the pairs of the head groups is 4–5 grid units. Also, the sharp peaks in the correlations indicate little variability in the arrangement of the *H*, *T*, and *I* groups on the surface.

For nonionic silane, we observe a higher fraction of *HH* correlations at distances of 1 and 2 grid units. The maxima in

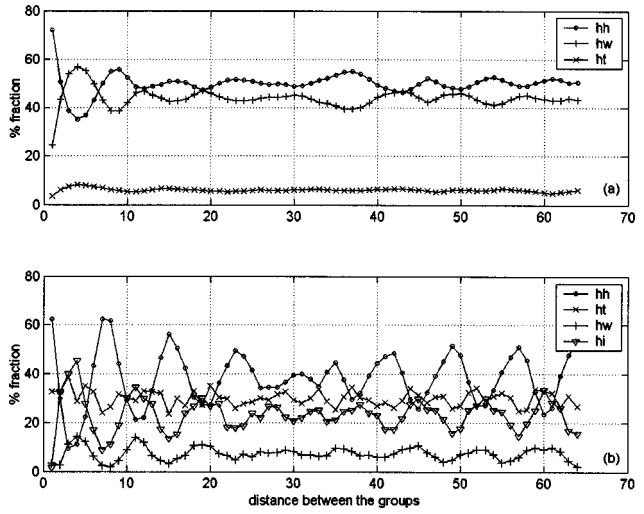

FIG. 5. (a) The *HH*, *HW*, and *HT* correlations in nonionic silane on layer 1, (b) the *HH*, *HW*, *HT*, and *HI* correlations in cationic silane on layer 1.

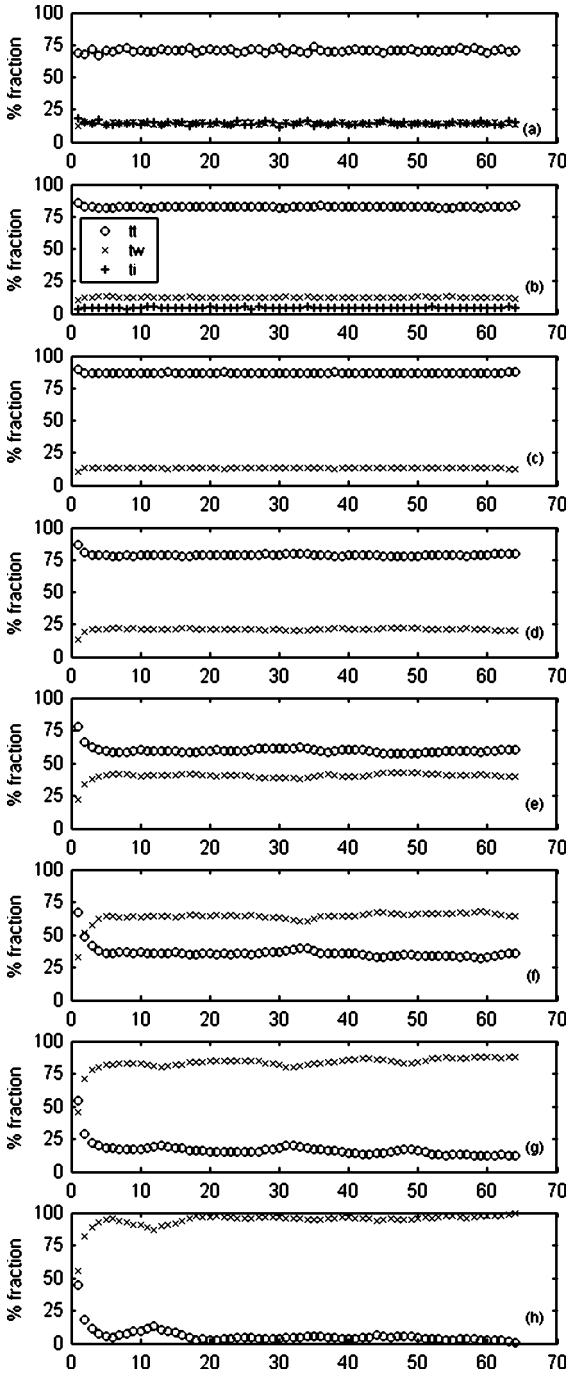

FIG. 6. *TT*, *TW*, and *TI* correlations on layers (a) 2, (b) 3, (c) 4, (d) 5, (e) 6, (f) 7, (g) 8, and (h) 9 of the cationic silane film.

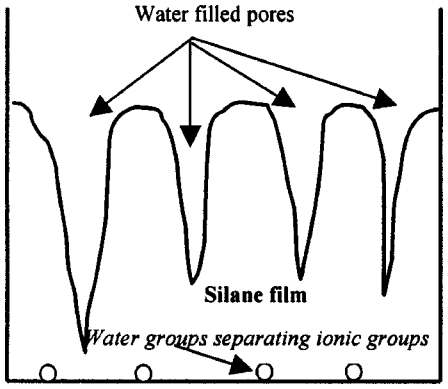

FIG. 7. A simplified representation of water pores in the deposited silane films.

HH correlations are observed at distances of 1, 8, 16, and 24 grid units with loss of definite correlations beyond. Also, the fraction of *HH* correlations stays larger than the *HW* and *HT* correlations at distances greater than 6 grid units. This suggests that the head groups in the nonionic silane attach to the surface sites in clusters of 3–5 groups. The correlations in Fig. 5(a) are not as sharp as in Fig. 5(b). This indicates more variability in the size and spacing between the clusters of *H* and clusters of *W* groups along the surface. The *HH* clusters are separated by pockets of water of 4 to 6 grid units in size. Some occasional presence of tail groups is also indicated by the *HT* correlations that could be ascribed to the random high-energy events in the simulations allowed by the transition probabilities. From the correlations of *HH* and *HW* the following structure of the nonionic silane is predicted on layer 1:

$$\underline{HHHH}WWW\underline{HHH}WWWW\underline{HHHHHH}WWW\ldots.$$

For determining the structure of the film beyond layer 1, we look at the *TW*, *TT*, and *TI* correlations in layers 2 through the top layer of the film. In Fig. 6, we show these correlations for ionic silane. In rinsed films, there is no ionic group present beyond layer 3. Similarly, negligible number of head groups is present in layers 2 and 3 which have been ignored for present analysis.

In Fig. 6(a), we observe oscillations in the *TT* correlations with a period of about 3–4 grid units. This suggests that the tail groups occupy the grid sites in layer 2 in groups of 3 or 4 with these groups separated by either an ionic group or the water group. The fraction of *TT* correlations in layers 3–5 is much higher than the fractions of *TW* and *TI* correlations. Therefore, these layers are predominantly packed with the tail groups. Also, the fraction of *TW* correlations in these layers, $R_{TW}^{i=3,4,5}(d)$, increases from $d=1$ to $d=3$ and then plateau. This indicates that the water groups are not dispersed and appear as a single cluster in this layer. Also, very low fraction of *TI* correlations in layers 2 and 3 indicates that these layers are depleted of ionic groups, which is expected as most of the ionic groups are adsorbed on layer 1. The *TT* and *TW* correlations beyond layer 5 again show a nonperiodic structure. This structuring can be related to the presence of several clusters of tail groups separated by clusters of water groups. Also, it is observed that water groups

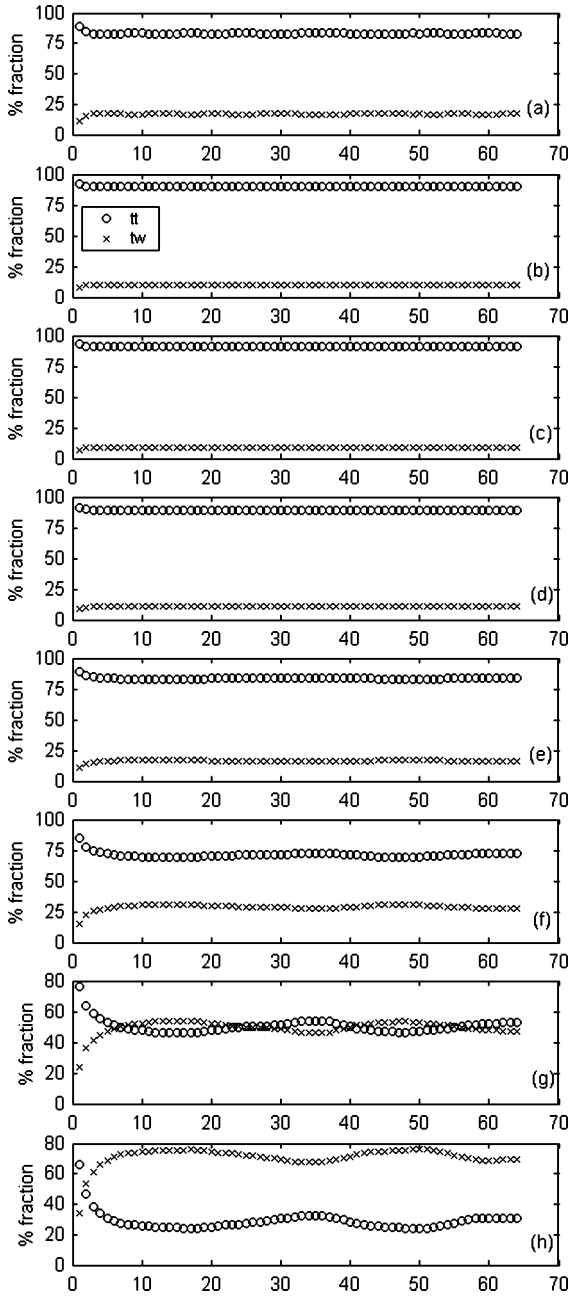

FIG. 8. *TT* and *TW* correlations in nonionic silane on layers (a) 2, (b) 3, (c) 4, (d) 5, (e) 6, (f) 7, (g) 8, and (h) 9.

become more predominant from layer 6 onwards. The presence of a single cluster of water groups in layers 2–4 and several clusters of water groups in layers 5 and 6 suggests that there could be at least one water filled pore in the film penetrating from the top surface of the film up to layer 3 and several other pores of water penetrating up to layer 5. To help visualization of these water pores, a schematic representation of the average deposited films with the water pores is shown in Fig. 7. Also, presence of pores in the ionic silane film can be seen in the snapshot shown in Fig. 2. The fraction of *TT* correlations, $R_{TT}^{i=7,8}(d)$, in Figs. 6(g) and 6(h) are seen to decrease from $d=1$ to $d=4$ with a still correlation at larger spacings. Therefore, tail groups in these layers are

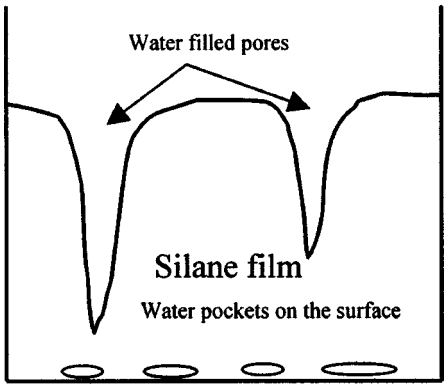

FIG. 9. A simplified representation of water filled pores in nonionic silane film.

expected to be present as cluster of 2–3 tail groups separated by water groups.

In Fig. 8, we show the *TT* and *TW* correlations in the nonionic silanes. From Fig. 8(a) through Fig. 8(e) we see that the *TW* correlations, $R_{TT}^{i=7,8}(d)$, increase from $d=1$ to $d=3$ and then plateau. Also, the fraction of *TT* correlations is observed to be much higher than fraction of *TW* correlations. Again, this indicates that these layers are mostly packed with the tail groups and water only appears as a single cluster of 3–4 water groups. In layers 6 through 9 we see progressively increasing levels of water. There is an early indication of structuring of tail and water groups in layers 6 and 7 that show a little peak between $d \in [30,40]$. This peak is more pronounced in layers 7 and 8. The correlation distance in Figs. 8(e)–8(h) suggests the presence of several clusters of the water groups separated by clusters of tail groups. Again, these correlations indicate that a water pore penetrates the film as deep as layer 2 and another water groove penetrates the film up to layer 5.

A simplified representation of these pores is shown in Fig. 9. Also, a look at layers 8 and below, in the snapshot of nonionic silane [Fig. 2(b)], will reveal that fewer water filled pores are present in this film compared to the cationic silane film. Since there are fewer peaks in the layers 7 and 8 in nonionic silane than in the case of ionic silane, we predict that the top surface of the deposited film is less rough in the nonionic silane films than in the case of ionic silane. Finally, in layer 8 the switch between the water fraction and the silane fraction is complete. The shape of the two curves in layer 8 suggests that the layer mostly occupied by water with very few tail groups.

CONCLUSIONS

The MC simulations in 2D were performed to investigate the effect of charged groups on the structure of nonionic and ionic silane films deposited on a hydrophilic surface from aqueous solutions. The films of ionic and nonionic silanes deposited on a hydrophilic surface were characterized by (i) calculating the distribution profiles of the head and tail groups as a function of distance from the surface, and (ii) spatial correlations between pairs of groups as a function of separation between the groups along the surface. Both the distribution profiles and spatial correlations indicate a higher porosity in the ionic silane films. Structures of simulated silane films are consistent with the measurement of the contact angles of the as-deposited uncured silane films.[35] Therefore, we expect equilibrium structures of nonionic and cationic silane films obtained from the simulations to represent the films that are obtained in the experiments prior to curing.

Simulations indicate that the morphology of the films is dictated by the topological constraints on the silanes anchoring at the surface sites. In our 2D simulations cationic silane chains are seen to anchor at two surface sites with the chemisorption of head groups and the physisorption of charged groups. Also, presence of cationic groups is noticed in layers closer to the surface. A low energy configuration in the cationic silane films is achieved by shielding of repulsive interactions between the cationic groups by a higher density of tail groups in the lower layers. This topology of the films in the lower layers also leads to higher porosity in the top layers of the cationic silane films. It is expected that this higher density of hydrophobic groups near the substrate is responsible for the higher contact angles seen for uncured cationic silane films in experiments.[8,9,35] In contrast, water pores have been observed in the layers closer to the substrate in the case of nonionic films.

Although, simulations have not been carried out to study the structures of the cured films, we speculate on the nature of the cured films based on the structures of the uncured films. Curing of the deposited films in experiments results in the removal of water trapped in the pores. Following the removal of water, the hydrophobic interaction, responsible for the folding of the hydrocarbon tail of silane in the aqueous environment, disappears. The hydrocarbon tails in the nonionic silane can, therefore, stretch out resulting in films terminated by terminal methyl groups. The methyl-terminated films have much higher contact angle than films that have methylene groups exposed.

As our simulations have been performed in two dimensions we refrain from making any direct quantitative comparisons between the simulated and the real systems. Despite the limitations of 2D systems in describing the real systems, important conclusions have been drawn from the structures of films obtained in our 2D simulations which are strikingly consistent with the experimental observations. We expect similar and more pronounced behavioral and structural features (porosity, etc.) for the systems in 3D.

ACKNOWLEDGMENT

The authors acknowledge the support of National Science Foundation (Grant No. 9905957 and Grant No. 0221865) for this work.

[1] U. Srinivasan, M. R. Houston, R. T. Howe, and R. Maboudian, J. Microelectromech. Syst. **7**, 252 (1998).
[2] R. L. Alley, G. J. Cuan, R. T. Howe, and K. Komvopoulos, IEEE Solid State Sensor and Actuator Workshop-Hilton Head '92, Hilton Head, South Carolina (1992), p. 202.
[3] N. Tas, T. Sonnenberg, H. Jansen, R. Legtenberg, and M. Elwenspoek, J. Micromech. Microeng. **6**, 385 (1996).

[4] M. R. Houston, R. Maboudian, and R. T. Howe, Solid state sensor and actuator workshop, Hilton Head, South Carolina, June 2–6, 1996, pp. 42–47.
[5] R. Maboudian, MRS Bull. **23**, 47 (1998).
[6] A. M. Almanza-Workman, S. Raghavan, P. Deymier, D. J. Monk, and R. Roop, Colloids Surf. A **232**, 67 (2004).
[7] A. M. Almanza-Workman, S. Raghavan, P. A. Deymier, D. J. Monk, and R. Roop, Ultra clean processing of silicon surfaces 2000, 2001, Oostende, Belgium, Vol. 76/77, pp. 23–26.
[8] A. M. Almanza-Workman, S. Raghavan, P. Deymier, D. J. Monk, and R. Roop, J. Electrochem. Soc. **149**, H6 (2002).
[9] A. M. Almanza-Workman, S. Raghavan, S. Petrovic, B. Gogoi, P. Deymier, D. J. Monk, and R. Roop, Thin Solid Films **423**, 77 (2003).
[10] S. Bandhopadhyay, J. C. Shelly, M. Tarek, P. B. Moore, and M. L. Klein, J. Phys. Chem. B **102**, 6318 (1998).
[11] H. Kuhn and H. Rehage, J. Phys. Chem. B **103**, 8493 (1999).
[12] H. Shinto, S. Tsuji, M. Miyahara, and K. Higashitani, Langmuir **15**, 578 (1999).
[13] L. Zhang, K. Wesley, and S. Jiang, Langmuir **17**, 6275 (2001).
[14] M. J. Stevens, Langmuir **15**, 2773 (1999).
[15] C. M. Wijmans and P. Linse, J. Phys. Chem. **100**, 12583 (1996).
[16] C. M. Wijmans and P. Linse, J. Phys. Chem. **106**, 328 (1997).
[17] C. Taut, A. J. Perstin, and M. Grunze, Langmuir **12**, 3481 (1996).
[18] R. G. Larson, L. E. Scriven, and H. T. Davis, J. Chem. Phys. **83**, 2411 (1985).
[19] R. G. Larson, J. Chem. Phys. **89**, 1642 (1988).
[20] R. G. Larson, J. Chem. Phys. **91**, 2479 (1989).
[21] R. G. Larson, J. Chem. Phys. **96**, 7904 (1992).
[22] R. G. Larson, Macromolecules **27**, 4198 (1994).
[23] K. Esselink, P. A. J. Hilbers, N. M. van Os, B. Smit, and S. Karaborni, Colloids Surf., A **91**, 155 (1994).
[24] S. Karaborni, K. Esselink, P. A. J. Hilbers, B. Smit, J. Karthauser, N. M. van Os, and R. Zana, Science **266**, 254 (1994).
[25] S. Karaborni, N. M. van Os, K. Esselink, and P. A. J. Hilbers, Langmuir **9**, 1175 (1993).
[26] J. C. Shelly, M. Y. Shelly, R. C. Reeder, S. Bandyopadhyay, and M. L. Klein, J. Phys. Chem. B **105**, 4464 (2001).
[27] S. J. Marrink and A. E. Mark, J. Am. Chem. Soc. **125**, 15233 (2003).
[28] V. Kapila, J. M. Harris, P. A. Deymier, and S. Raghavan, Langmuir **18**, 3728 (2002).
[29] A. W. Adamson, *Physical Chemistry of Surfaces* (Wiley, New York, 1982).
[30] P. C. Hiemenz, *Principles of Colloid and Surface Chemistry* (Dekker, New York, 1997).
[31] P. Linse and H. C. Andersen, J. Chem. Phys. **85**, 3027 (1986).
[32] A. V. Shevade, S. Jiang, and K. E. Gubbins, Mol. Phys. **97**, 1139 (1999).
[33] A. V. Shevade, S. Jiang, and K. E. Gubbins, J. Chem. Phys. **113**, 6933 (2000).
[34] B. Smit and D. Frenkel, *Understanding Molecular Simulations: From Algorithms to Applications*, 2nd ed. (Academic, San Diego, 2002).
[35] A. M. Almanza-Workman, Ph.D. dissertation, University of Arizona, Tucson, AZ, 2002.